

## Use of hen feathers to remove Reactive Black 5 and Basic Red 46 from aqueous solutions

Tomasz Józwiak\*, Urszula Filipkowska, Patryk Marciniak

Department of Environmental Engineering, University of Warmia and Mazury in Olsztyn, Warszawska St. 117a, 10-957 Olsztyn, Poland, emails: tomasz.jozwiak@uwm.edu.pl (T. Józwiak), urszula.filipkowska@uwm.edu.pl (U. Filipkowska), patrykmarciniak139@gmail.com (P. Marciniak)

Received 5 March 2021; Accepted 11 June 2021

---

### ABSTRACT

This study aimed to determine the effectiveness of Reactive Black 5 (RB5) and Basic Red 46 (BR46) sorption on hen feathers (HF), being a post-slaughter waste from the poultry industry. The scope of the study included, i.a. FTIR spectra analysis of hen feathers, pH effect on dye sorption effectiveness, dye sorption kinetics (pseudo-first order model, pseudo-second order model, intramolecular diffusion model), and maximal sorption capacity of the sorbent (Langmuir 1 and 2 models, and Freundlich model). The effectiveness of RB5 sorption onto HF was the highest at pH 2 and that of BR46 – at pH 5. The time needed to reach RB5 and BR46 sorption equilibrium onto HF ranged from 180 to 210 min. The kinetics of dye sorption onto HF was best described by the pseudo-first order model, which indicates the typically physical nature of the sorption process. The constants determined from the intramolecular diffusion model demonstrated that RB5 and BR46 sorption onto HF proceeded in two main phases, differing in sorption intensity. The maximal sorption capacity of HF reached 5.19 mg/g for RB5 and 4.06 mg/g for BR46. The identical values of  $K_C$ ,  $K_1$ , and  $K_2$  constants determined from the Langmuir 1 and Langmuir 2 models suggest that only one type of the sorption center played the key role in the sorption process.

*Keywords:* Sorption; Unconventional sorbent; Hen feathers; Reactive Black 5; Basic Red 46

---

### 1. Introduction

Insufficiently treated wastewater discharged to surface waters poses a severe threat to the aquatic environment. Especially hazardous in this respect are spent waters from plants of the textile, tanning, or paper industries. Their high nuisance stems from the presence of dyes, which cause risk to the environment even in minor concentrations. Dyes present in natural waters block the access of sun-rays to aquatic plants, thus inhibiting the photosynthesis process [1]. They also impair oxygen diffusion in water, which may lead to the appearance of anaerobic zones. Finally, dyes and products of their degradation can be toxic to organisms inhabiting water reservoirs [2].

To recapitulate, the color wastewater that pervaded the natural environment can cause the ecosystem to break down. The necessity of environmental protection urges the search for efficient methods for wastewater decolorization.

Color wastewater treatment with traditional biological methods is quite challenging due to the low biodegradability of dyes because of the aromatic rings in their structure [3]. For this reason, physicochemical methods are recommended instead. They include, for example, coagulation, membrane techniques (including ultrafiltration and reversed osmosis), advanced chemical oxygenation (including ozonation or Fenton's reaction) [4] or photocatalytic degradation [5,6]. However, most of these processes are costly or generate intermediate toxic products. For this reason, high interest has recently been

---

\* Corresponding author.

spurred by the decolorization methods based on dye sorption as an environmentally-friendly process, the cost and effectiveness of which are predicated by sorbent type.

Sorbents based on activated carbons are commonly used for industrial wastewater decolorization. They are produced upon the carbonization and activation of organic materials, such as, peat or wood. These sorbents' hallmark feature is their very large surface reaching even up to 2,000–2,500 m<sup>2</sup>/g [7]. Their advantages also include excellent sorption properties regarding most commercial dyes and the possibility of their regeneration after use. In contrast, a significant drawback of activated carbons is their relatively high price, which necessitates the search for their cheaper replacers.

Today, high hopes are fostered in using waste materials from the agri-food industry for sorbent production. Industrial wastes, both these of plant and animal origin, are usually widely available in each country and, therefore, cheap.

The possibility of using waste plant biomass as a sorbent is mainly due to its polysaccharides (cellulose and hemicellulose) and lignin. These components ensure good sorption properties of plant materials in respect of cationic dyes. The production process of biosorbents from plant biomass is usually not complicated and often limited to its purification, drying, and disintegration. The plant-derived sorbents investigated thus far include, i.a., nutshells (e.g., coconuts [8], walnuts [9], or peanuts [10]), cereal grain hulls (e.g., rice [11], oats [12], or wheat [13]), corn cobs [14], fruit skins (e.g., bananas or citrus fruits [15]) or vegetable peels (e.g., cucumbers or potatoes [16]). A drawback of most biosorbents based on plant-derived waste material is their generally acidic character, responsible for the low sorption effectiveness of anionic dyes (acidic and reactive ones).

The animal biomass-based sorbents offer an alternative to those based on plant biomass. Waste products from processing sea crustaceans, including exoskeletons of shrimps, crabs, or lobsters, are extremely popular in this respect. They are rich in chitin, that is, a polysaccharide precursor of chitosan [17]. Both chitin and chitosan are highly capable of anionic dye binding. Hydrogel forms of chitosan may exhibit even several times higher sorption capacity than commercial sorbents based on activated carbons [18]. However, a drawback of the "high-chitin" materials is the depletion of their market resources due to their purchase by pharmaceutical companies to produce dietary supplements.

Other waste materials of animal origin used for sorbent production include high-calcium materials, such as, eggshells [19] and animal bones [20]. However, they are usually digested at low pH (pH < 3), which eliminates their usability for the treatment of acidic wastewater from the textile industry.

An example of a widely-available animal-derived material that remains stable in a wide range of pH values is poultry feathers. They are the post-slaughter waste material from poultry pre-treatment. Considering the vast popularity of poultry meat as a crucial component in man's diet, feathers recovered become a widely-available and cheap material, with their annual global production estimated to exceed 4 million tonnes [21]. The main building material of feathers is keratin, which accounts for over 90% of their entire structure [22]. Despite their protein structure, feathers represent a stable material, relatively resistant to the action of both

physical and biological factors. Owing to their acidic functional groups (e.g., carboxyl groups) and alkaline functional groups (e.g., amine groups), they are potentially suitable sorbents of both anionic and cationic dyes.

This study aimed to examine the potential feasibility of hen feathers as a sorbent to remove dyes from aqueous solutions. The following dyes, popular in the textile industry, were used as sorbates: Reactive Black 5 (anionic, reactive) and Basic Red 46 (cationic), which, according to the authors' knowledge, have not yet been tested on feather-based sorbents.

## 2. Materials and methods

### 2.1. Hen feathers

Feathers of hen broilers of Cobb 500 breed were used as a sorbent in the study. They were provided by a poultry slaughterhouse located in the Warmia and Mazury Province (northern Poland). The hen feathers were composed of keratin (92.9%–96.4%), lipids (0.9%–1.1%), and other components (saccharides, ashes) (2.5%–6.2%) [22,23]. The sorbent prepared for the research had a surface area of 31, 5–33, 6 m<sup>2</sup>/g.

### 2.2. Dyes

The sorption properties of hen feathers were tested using dyes popular in the textile industry: Reactive Black 5 (RB5) and Basic Red 46 (BR46), purchased from a dye producing plant "BORUTA S.A." (Zgierz, Poland). The characteristics of dyes tested are presented in Table 1.

### 2.3. Laboratory equipment

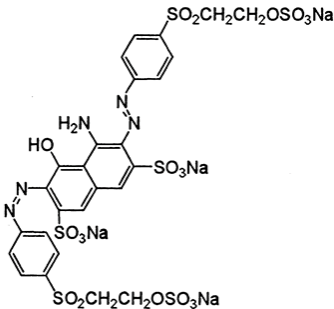
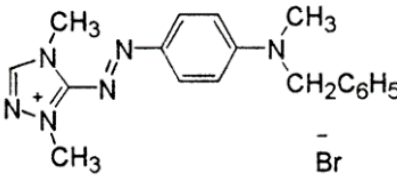
The following laboratory equipments were used in the study:

- HI 110 pH meter, HANNA Instruments, Poland – (solution pH correction),
- Multi-Channel Stirrer MS-53M, JEIO TECH, Korea – (dye sorption analyses),
- Multi-station MS-53M Magnetic Stirrer, GMI, USA – (dye sorption analyses),
- UV-3100 PC spectrophotometer, VWR spectrophotometers, Canada – (determination of dye concentration in the solution),
- FT/IR-4700LE FT-IR Spectrometer with single reflection ATR attachment– JASCO INTERNATIONAL, Japan – (preparation of sorbent FTIR spectra),
- BET surface analyzer - AUTOSORB-1 - QuantaChrome Corporation, USA – (measurement of the surface area of sorbents).

### 2.4. Preparation of sorbents

Hen feathers of 1.0–2.0 cm in length were selected for the study. They were rinsed with hot distilled water (temperature of 75°C–80°C) on a laboratory screen and afterward dried in a laboratory drier at a temperature of 105°C. Thus prepared hen feathers (HF) were stored in air-tight plastic containers at a room temperature (22°C).

Table 1  
Characteristics of Reactive Black 5 and Basic Red 46

Dye type	Reactive Black 5 (RB5)	Basic Red 46 (BR46)
Structural formula		
Molecular formula	$C_{26}H_{21}N_5Na_4O_{19}S_6$	$C_{18}H_{21}BrN_6$
Molecular weight	991.8 g/mol	401.3 g/mol
Dye class	Double azo dye	Single azo dye
Dye type	Anionic (reactive)	Cationic
Absorption maximum ( $\lambda_{max}$ )	600 nm	530 nm
Uses	Dyeing cotton, wool, and polyamide fibers	Dyeing leather, paper, wool, and acrylic fibers
Hazards	Irritating the respiratory tract, causing allergic reactions	Caustic, toxic, hazardous to the aquatic environment

### 2.5. Analyses of pH effect on dye sorption effectiveness

Dye solutions with the concentration of 50 mg/L and pH values in the subsequent solutions reaching: 2.0/3.0/4.0/5.0/6.0/7.0/8.0/9.0/10.0/11.0 were prepared in measuring flasks (100 mL). Their pH was corrected with appropriate doses of 0.1/1.0 M HCl or NaOH. The HF were weighed in portions of 0.5 g d.m. using a precise scale to a series of conical flasks (250 mL). Then, the earlier prepared dye solutions (100 mL) were added to the flasks, which were placed on a laboratory shaker (150 rpm, 30 mm vibration amplitude). After 120 min, samples (10 mL) were collected with an automatic pipette from each flask. The concentration of dye left in the solution was determined with the spectrophotometric method using a UV-VIS SP3100 spectrophotometer (at the wavelengths of 600 nm for RB5 and 530 nm for BR46). Determinations were performed using 10 mm quartz measuring cuvettes. The pH value of the solutions after the sorption process was measured as well.

### 2.6. Analyses of dye sorption kinetics

Solutions with dye concentrations of 10/50/100 mg/L and optimal pH value (established as in point 2.5) were prepared in measuring flasks (1,000 mL). Then, 5 g d.m. of HF were weighed using a precise scale to a series of beakers (1,000 mL). The earlier prepared dye solutions (1,000 mL) were added to these beakers, which were next transferred onto a multi-station magnetic stirrer (150 rpm). In the set time intervals (i.e., after 0, 10, 20, 30, 45, 60, 90, 120, 150, 180, 210, 240, and 300 min), 5 mL samples were collected from the solutions with an automatic pipette. The concentration of dyes in the collected samples was determined with the spectrophotometric method (described in Section 2.5).

### 2.7. Analyses of the maximal sorption capacity

Solutions with dye concentrations of 5, 10, 20, 30, 40, 50, 60, 70, 80, 100 mg/L and optimal pH value (established as in point 2.5) were prepared in measuring flasks (100 mL). Then, 0.5 g d.m. of HF were weighed using a precise scale to a series of beakers (250 mL). The earlier prepared dye solutions (100 mL) were added to these beakers, which were next placed on a shaker (150 rpm, 30 mm vibration amplitude). Once the time needed to reach sorption equilibrium (established in point 2.6) had been reached. Samples (10 mL) were collected from each flask to the earlier prepared test tubes for the spectrophotometric determination of the concentration of dye left in the solution.

### 2.8. Computational methods

The amount of dye adsorbed onto HF was determined using Eq. (1):

$$Q_s = (C_0 - C_s) \times \frac{V}{m} \quad (1)$$

where  $Q_s$  – mass of sorbed dye [mg/g d.m.];  $C_0$  – initial dye concentration [mg/L];  $C$  – concentration of dye left in the solution after the sorption process [mg/L];  $V$  – solution volume [L];  $m$  – sorbent mass [g d.m.].

The kinetics of dye sorption onto HF was described using the pseudo-first order model (2), the pseudo-second order model (3), and the intramolecular diffusion model (4).

$$\frac{\Delta q}{\Delta t} = k_1 \times (q_e - q) \quad (2)$$

$$\frac{\Delta q}{\Delta t} = k_2 \times (q_e - q)^2 \quad (3)$$

$$q = k_{id} \times t^{0.5} \quad (4)$$

where  $q_e$  – equilibrium amount of sorbed dye [mg/g],  $Q$  – instantaneous mass of adsorbed dye [mg/g],  $k_1$  – sorption rate constant in the pseudo-first order model [1/min];  $k_2$  – sorption rate constant in the pseudo-second order model [1/min];  $k_{id}$  – sorption rate constant in the intramolecular diffusion model [mg/g min<sup>0.5</sup>];  $t$  – sorption time [min].

The experimental data obtained from the analyses of the maximal sorption capacity were described using three adsorption isotherms: Langmuir 1 isotherm (5), Langmuir 2 isotherm (6), and Freundlich isotherm (7).

$$q_e = \frac{(q_{max} \times K_c \times C)}{(1 + K_c \times C)} \quad (5)$$

$$q_e = \frac{(b_1 \times K_1 \times C)}{(1 + K_1 \times C)} + \frac{(b_2 \times K_2 \times C)}{(1 + K_2 \times C)} \quad (6)$$

$$q_e = K \times C^n \quad (7)$$

where  $q_e$  – equilibrium amount of sorbed dye [mg/g],  $q_{max}$  – maximal capacity of the monolayer [mg/g],  $b_1$  – maximal capacity of type I active sites in the monolayer [mg/g],  $b_2$  – maximal capacity of type II active sites in the monolayer [mg/g],  $k_1/k_2$  – constants in the double Langmuir equation [L/mg],  $K$  – constant of the sorption equilibrium in the Freundlich equation,  $C$  – concentration of dye left in the solution after the sorption process [mg/L],  $n$  – heterogeneity parameter (Freundlich model).

### 3. Results and discussion

#### 3.1. FTIR analysis of hen feathers

The spectrometric spectrum of the hen feathers (HF) tested was typical of keratinic materials (Fig. 1). It revealed characteristic bands of peptide bonds (–CONH), known as Amide A (3,500–3,200 cm<sup>−1</sup>), Amide B (3,100–3,020 cm<sup>−1</sup>), Amide I (1,700–1,600 cm<sup>−1</sup>), Amide II (1,580–1,510 cm<sup>−1</sup>), and Amide III (1,320–1,200 cm<sup>−1</sup>) [24]. A wide band of Amide A corresponded to the stretching of the O–H and N–H bonds (peak at 3,250 cm<sup>−1</sup>). The peak of N–H band (3,060 cm<sup>−1</sup>) was also present in the band of Amide B [25]. A distinct peak at 1,620 cm<sup>−1</sup> in the Amide I band pointed to the stretching of the C=O bond, whereas the peak at 1,510 cm<sup>−1</sup> in the Amide II band suggested stretching vibrations of the C–N bond. The presence of C=O and C–N was also indicated by the peaks at 1,310 and 1,230 cm<sup>−1</sup> visible in the spectral band of Amide III [26]. A series of peaks at 2,960; 2,920; 2,870 and 2,850 cm<sup>−1</sup> corresponded to the asymmetric and symmetric stretching vibrations of CH<sub>2</sub> and CH<sub>3</sub>, belonging to the lipid chains, and also protein terminal groups. The vibrations of the lipid bonds CH<sub>2</sub> and CH<sub>3</sub> were also indicated by the peaks at 1,340 and 1,445 cm<sup>−1</sup> [27]. The peak at 1,385 cm<sup>−1</sup> corresponded to the stretching of the C–O bond, whereas a

series of small peaks at 1,125; 1,056 and 1,040 cm<sup>−1</sup> pointed to C–C skeletal stretches [27] (Fig. 1).

#### 3.2. Effect of pH on the effectiveness of dye sorption onto HF

The effectiveness of RB5 sorption onto HF was the highest at pH 2 and decreased along with pH increase, reaching the lowest value at pH 11. The greatest decrease in RB5 sorption effectiveness was observed at pH 2–5 and pH 10–11, whereas in the initial pH range of 5–9, the effectiveness of dye sorption was similar (Fig. 2a).

These tendencies obtained for RB5 dye are due to a high content of protein (keratin) in the feathers, rich in amine and carboxyl functional groups. At pH < 9, most of the secondary amine groups (–NHR) occur in the protonated form (–NH<sub>2</sub>R<sup>+</sup>) in the chemical structure of proteins. In turn, at pH > 4, most of the carboxyl functional groups of keratin occur in the deprotonated form (–COO<sup>−</sup>). Each protonated amine functional group generates a local positive electric charge, while each deprotonated group generates a local negative charge on sorbent surface. At pH 2, the number of protonated amine groups significantly surpasses the number of deprotonated carboxyl groups, which results in the total positive charge generated on feather surface. The positively charged surface of the sorbent attracts electrostatically RB5 anions, which significantly facilitates their sorption. This explains the high effectiveness of RB5 binding onto HF at low pH values. With pH increase, the ratio of the number of functional groups generating the positive charge to that of the groups generating the negative charge decreases. At pH > 5, practically all carboxyl groups possessed a negative charge, which resulted in the neutralization of the electric charge on sorbent surface. This explains the tangible decrease in the effectiveness of RB5 sorption onto HF along with pH increase, observed at pH 2–5 (Fig. 2a). In the pH range of pH 5–9, the number of protonated and deprotonated functional groups of keratin remained at a similar level, contributing to the similar electric charge and, ultimately, similar RB5 sorption effectiveness. At pH > 9, the number of deprotonated carboxyl groups started to surpass the number of protonated amine groups, resulting in the total negative charge of the sorbent. The negatively charged surface of HF repulsed electrostatically the anionic dye RB5, which resulted in a significant decrease in its sorption effectiveness. At pH 11, the negative charge on sorbent surface was large enough to make RB5 binding with HF practically impossible.

A similar pH effect on RB5 sorption was also observed in the studies reporting wastewater decolorization onto sorbents based on chitosan [28], sunflower seed husks [29], and activated carbon [30].

The effectiveness of BR46 sorption onto HF increased along with the initial pH increasing, reaching the highest value at pH 5 (Fig. 2a). The greatest changes in dye sorption effectiveness were noted at pH 2–5. The intensity of BR46 onto the keratinic sorbent was similar in the pH range of pH 5–6. At pH 6–9, any increase in the pH value resulted in a noticeable decrease in the effectiveness of dye binding onto HF. Due to the spontaneous decolorization of the dye solution at pH > 8 and to the risk of data misinterpretation, the

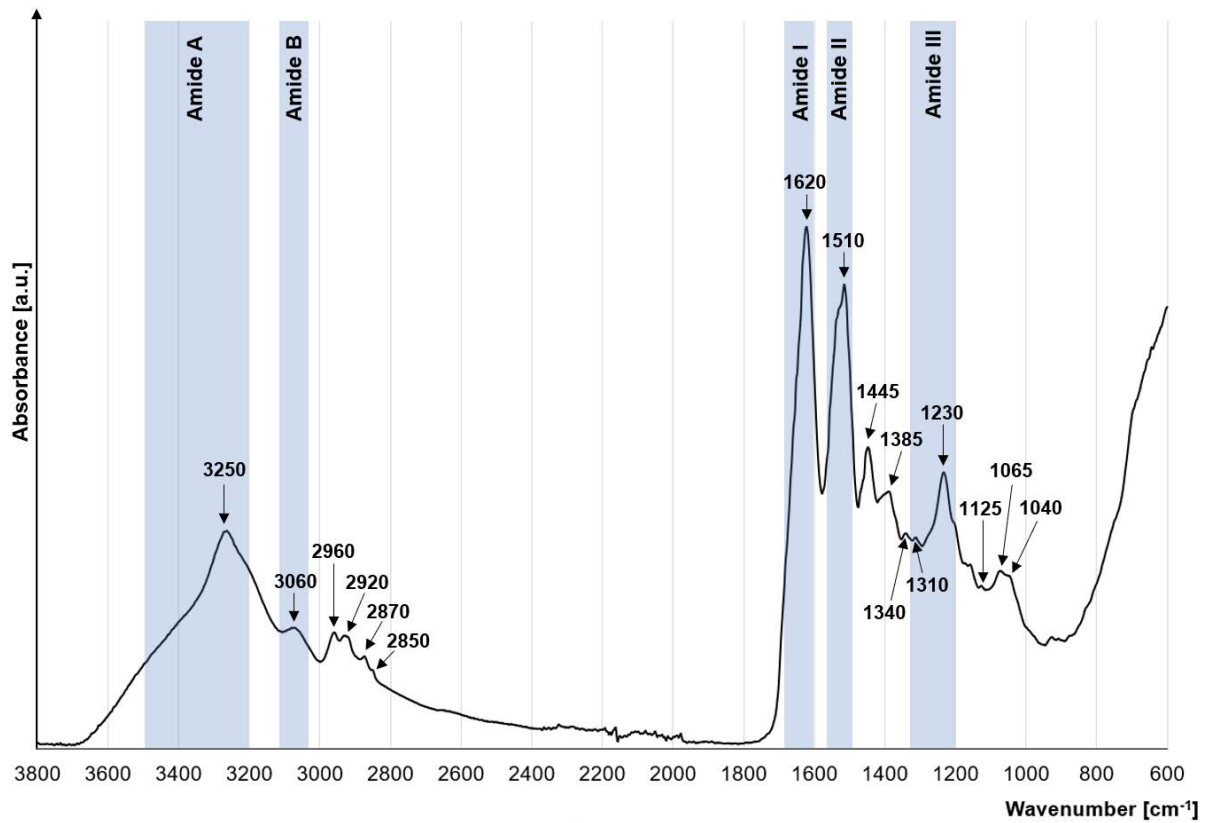


Fig. 1. FTIR spectra of HF.

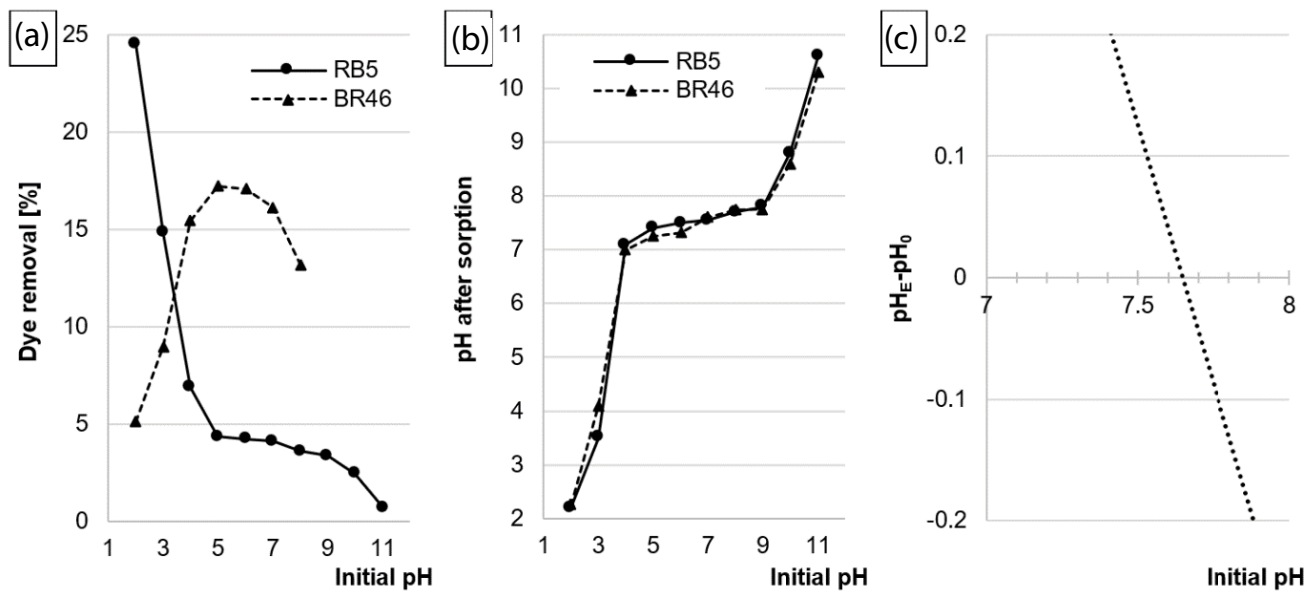


Fig. 2. (a) Effect of pH on the effectiveness of dye sorption onto HF. (b) Effect of HF on changes in pH values of the solutions during sorption. (c) Determination of  $pH_{E-pH_0}$  of the sorbents tested with the Boehm's titration method. Temperature 22°C.

results of BR46 sorption onto HF achieved at initial pH 9–11 were not presented graphically (Fig. 2a).

Unlike RB5, BR46 is alkaline in nature and dissociates in aqueous solutions, generating color cations. At low pH (pH 2), at which the HF surface has a strong

total positive charge, this sorbent repulses electrostatically dye cations, which contributes to its low sorption effectiveness. As mentioned earlier, the positive electric charge on sorbent surface decreases with pH increase. At pH > 4, the electric charges generated by amine and

carboxyl groups of HF begin to neutralize, thus reducing the effect of electrostatic repulsion between the dye and sorbent surface, and ultimately promoting effective BR46 binding onto HF. This explains the ramp of dye sorption effectiveness observed at pH 2–5 in Fig. 2a BR46 possesses tertiary amine groups responsible for its cationic character. At pH > 7, a part of its amine groups become deprotonated, contributing to the loss of the positive charge. This loss may, in turn, be reflected in the poorer dye interaction with the sorbent, which explains the reduced effectiveness of BR46 sorption onto HF at pH 7–9.

A similar pH effect on BR46 sorption was reported in studies addressing dye sorption onto coconut shells [8], graphene [31], and biomass of *Pleurotus mutilus* fungus [32]. The authors of the above-mentioned studies also point to a significant role of the sorbent surface charge in the sorption process (physical sorption) of BR46 and to the minor effect of chemisorption on the ultimate result.

The HF was observed to cause significant changes in dye solution pH during the sorption process. At the initial pH 4–9, the pH values of RB5 and BR46 sorption onto HF fixed in the range of pH 7.0–7.7 (Fig. 2b). The system with the solution containing hen feathers tended to reach the pH value approximating their  $pH_{pZC}$  ( $pH_{pZC:PK} = 7.65$  – Fig. 2c).

The successive stages of investigations into dye sorption onto HF (sorption kinetics, maximal sorption capacity) were carried out at sorption pH optimal for each dye (i.e., pH 2 for RB5 and pH 5 for BR46).

### 3.3. Kinetics of dye sorption onto HF

The time needed to reach RB5 and BR46 sorption equilibrium onto HF ranged from 180 to 210 min (Fig. 3). The intensity of dye sorption was found to be the highest in the initial phases of the sorption process. Already after 30 min of sorption, the amount of RB5 bound with HF ranged from 54.0% to 61.9% of  $q_e$  value (amount of dye

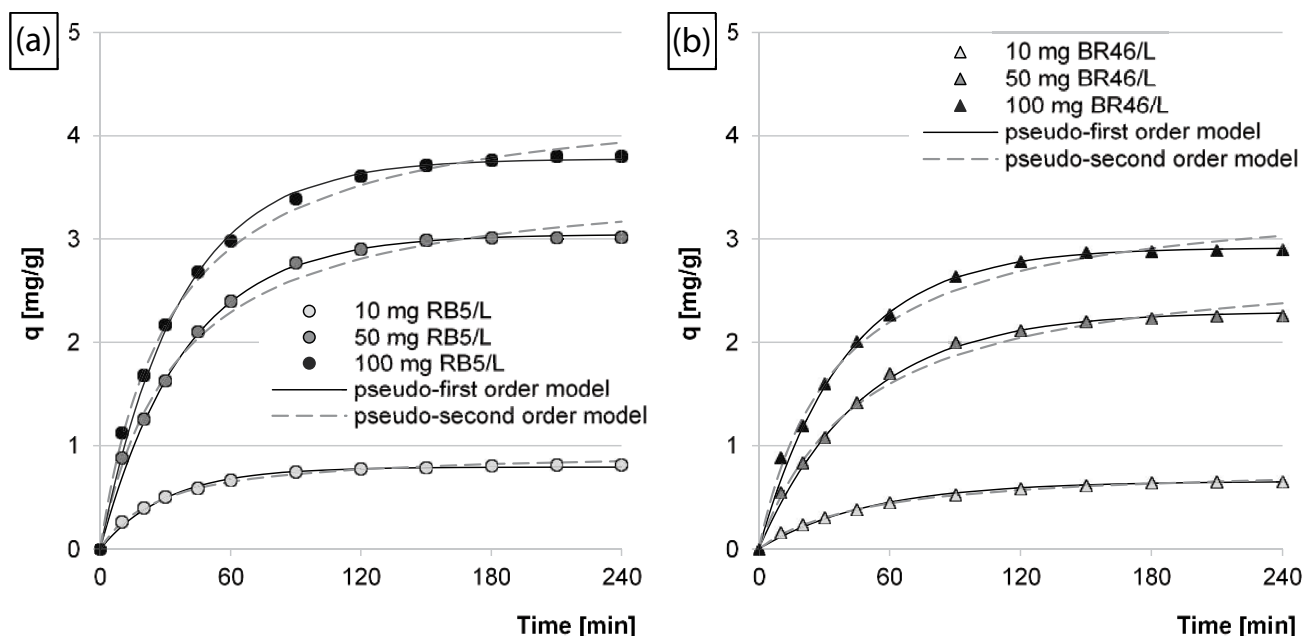


Fig. 3. Kinetics of sorption of (a) RB5; (b) BR46 onto HF. The pseudo-first order model and the pseudo-second order model. Temperature 22°C.

Table 2

Kinetic parameters of RB5 and BR46 sorption onto HF determined from the pseudo-first order model and pseudo-second order model

Dye	Dye conc. [mg/L]	Equilibrium time [min]	Exp. data $q_{e,exp}$ [mg/g]	Pseudo-first order model			Pseudo-second order model		
				$k_1$ [1/min]	$q_{e,cal}$ [mg/g]	$R^2$	$k_2$ [g/mg min]	$q_{e,cal}$ [mg/g]	$R^2$
RB5	10	210	0.814	0.0255	0.793	0.9980	0.0383	0.949	0.9967
	50	210	3.019	0.0273	3.044	0.9995	0.0078	3.632	0.9895
	100	180	3.773	0.0324	3.777	0.9984	0.0070	4.460	0.9940
BR46	10	180	0.652	0.0195	0.655	0.9974	0.0247	0.811	0.9947
	50	180	2.260	0.0211	2.299	0.9978	0.0086	2.840	0.9879
	100	180	2.900	0.0226	2.916	0.9993	0.0083	3.473	0.9910

bound with the sorbent after equilibrium time). The quantity of BR46 bound after the same time was similar and ranged from 47.6% to 55.7% of  $q_e$ .

The higher dye sorption effectiveness at the beginning of the sorption process is a typical phenomenon. The higher dye concentration at beginning of the reaction and the higher number of free active sites contributed to the higher likelihood of sorbate molecules colliding with sorption centers and, ultimately, to the higher sorption rate [33]. The concentration of sorbate and the number of free active sites decreased over the sorption process, leading to the corresponding decrease in the sorption rate with time (Fig. 3).

A similar RB5 sorption equilibrium time was also obtained in the studies into the treatment of aqueous solutions onto sunflower seed husks (210 min) [34], wheat straw (195 min) [35], and commercial activated carbons [36]. In the case of BR46, a similar sorption equilibrium time was also achieved in the studies reporting dye sorption onto pumpkin seed husks (180 min) [37] and skins of citrus fruits (180–240 min) [38]. The relative short equilibrium time of

RB5 and BR46 sorption onto HF (<12 h) suggests a relatively compact sorbent structure impairing dye penetration to the deeper layers of the sorbent. Presumably, RB5 and BR46 sorption onto HF was mainly due the adsorption process.

The experimental data obtained in the study were described with the pseudo-first order and pseudo-second order models (Table 2, Fig. 3). The values of the coefficient of determination ( $R^2$ ) computed using these models indicate that the pseudo-first order model showed the best fit to the data obtained for both dyes, irrespective of their initial concentrations. This shows that RB5 and BR46 binding onto HF was mainly attributed to the physical adsorption [39]. In the case of the sorption process of both RB5 and BR46, the  $q_e$  values determined from the pseudo-first order model increased along with the increasing initial dye concentration. This may point to the low affinity of dye to HF sorption centers. The increase in the values of sorption rate constants ( $k_1$ ) along with higher initial dye concentration may be explained by the greater likelihood of sorbate molecule collisions with HF active sites at higher dye concentrations.

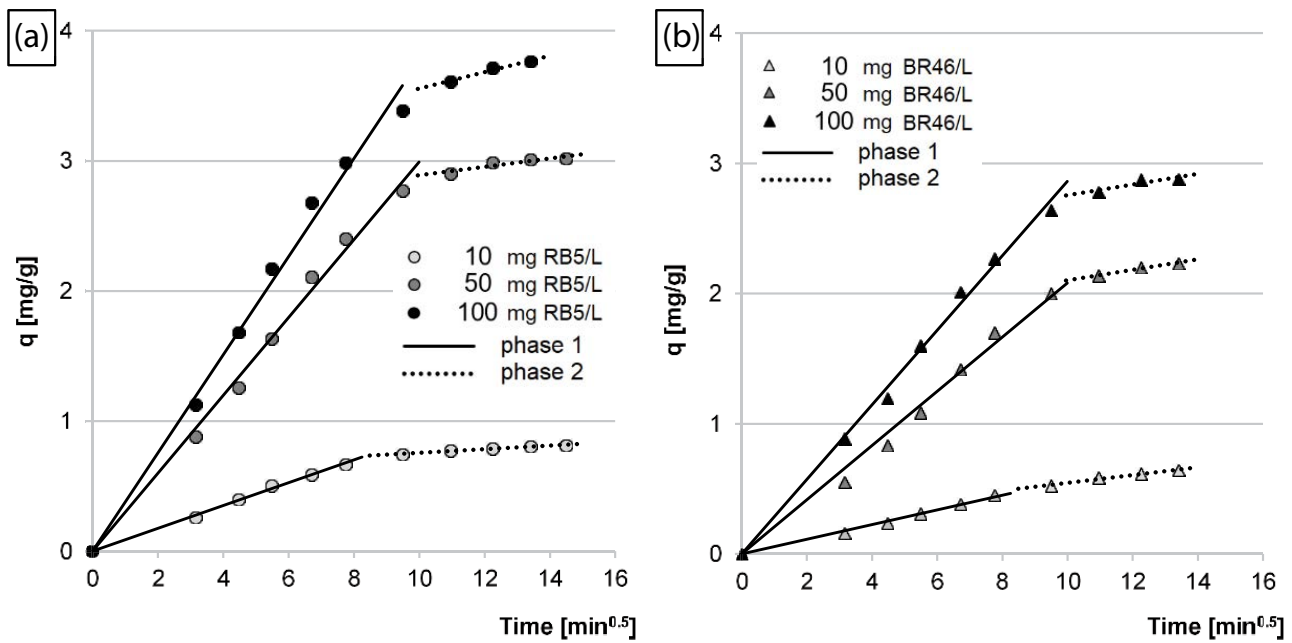


Fig. 4. Intramolecular diffusion model of sorption of: (a) RB5; (b) BR46 onto HF. Temperature 22°C.

Table 3  
Rate constants of RB5 and BR46 diffusion determined from a simplified intramolecular diffusion model

Dye	Dye conc. [mg/L]	Phase I			Phase II		
		$k_{d1}$	Duration	$R^2$	$k_{d2}$	Duration	$R^2$
RB5	10	0.0878	~60	0.9992	0.0136	~150	0.9661
	50	0.2994	~90	0.9986	0.0319	~120	0.9389
	100	0.3773	~90	0.9979	0.0633	~90	0.9752
BR46	10	0.0566	~60	0.9978	0.0302	~120	0.9736
	50	0.2082	~90	0.9971	0.0399	~90	0.9772
	100	0.2864	~90	0.9988	0.0403	~90	0.8272

Units:  $k_{d1}, k_{d2}, k_{d3}$  = [mg/g min<sup>0.5</sup>], duration [min],  $R^2$  [-]

The constants determined from the intramolecular diffusion model demonstrated that RB5 and BR46 sorption onto HF proceeded in two main phases differing in sorption intensity (Fig. 4; Table 3). In phase I, the dye diffused from the solution onto the sorbent surface and occupied the most accessible sorption centers. In phase II, dye molecules occupied the remaining sorption centers on HF surface and penetrated to the active sites located in deeper sorbent layers. Due to the initially higher number of free active sites and the higher number of sorbate molecules in the solution, phase I was characterized by a higher dye sorption intensity than phase II.

The phase I of RB5 and BR46 sorption onto HF lasted from 60 min (at dye concentration of 10 mg/L) to 90 min (at 50 and 100 mg/L). The faster appearance of phase II in the experimental series with the lowest initial dye concentration can be explained by faster depletion of dye molecules available in the solution. The  $k_{d1}$  and  $k_{d2}$  constants (indicating sorption intensity) determined from the model increased along with the increasing dye concentration, which - as in the case of sorption rate constants ( $k_1$ ) - can be explained by the increasing probability of collisions of dye molecules with sorption centers.

### 3.4. Maximal sorption capacity of HF

The experimental data obtained from the analyses of the maximal sorption capacity of HF regarding RB5 and BR46 dyes were described using the Langmuir 1 isotherm,

Langmuir 2 isotherm, and Freundlich isotherm (Table 4, Fig. 5). The Langmuir 1 and Langmuir 2 isotherms showed better fit to the experimental data compared with the Freundlich isotherm. This suggests that RB5 and BR46 dyes form a monolayer on HF surface and that single sorption centers can bind only one dye molecule. The  $K_c/K_1/K_2$  values (i.e., values of the affinity index) determined from Langmuir 1 and Langmuir 2 models for RB5 and BR46 were identical. This may point to the key role of only one type of the sorption center during dye binding. Presumably, the protonated tertiary amine group of keratin was the key sorption center for RB5, whereas the deprotonated carboxyl group of keratin - for BR46.

Despite various chemical natures of the dyes and various sorption pHs tested, the maximal sorption capacity of HF was similar in the case of both dyes and reached 5.19 mg/g for RB5 and 4.06 mg/g for BR46. Also the index of dye affinity to the active center was similar for both dyes ( $K_c = 0.035$  for RB5 and  $K_c = 0.030$  for BR46). The above data point to the versatility of hen feathers as a sorbent and to the possibility of using it to treat various types of color wastewater.

Table 5 compares sorption capacities of hen feathers, other unconventional sorbents, and selected commercial sorbents.

The sorption capacity of HF is inferior to that of the sorbents based on activated carbons [41,42,48,49], which is presumably due to its smaller specific surface. The HF also shows lower capability to bind the cationic dye BR46

Table 4  
Constants determined from the Langmuir 1 model, Langmuir 2 model and Freundlich model

Dye	Langmuir 1			Langmuir 2						Freundlich		
	$Q_{\max}$	$K_c$	$R^2$	$Q_{\max}$	$b_1$	$K_1$	$b_2$	$K_2$	$R^2$	$k$	$n$	$R^2$
	[mg/g]	[L/mg]	-	[mg/g]	[mg/g]	[L/mg]	[mg/g]	[L/mg]	-	-	-	-
RB5	5.191	0.0530	0.9919	5.191	3.313	0.0350	1.878	0.0350	0.9919	0.4389	0.5087	0.9504
BR46	4.061	0.0300	0.9968	4.061	1.945	0.0300	2.116	0.0300	0.9968	0.3062	0.5213	0.9701

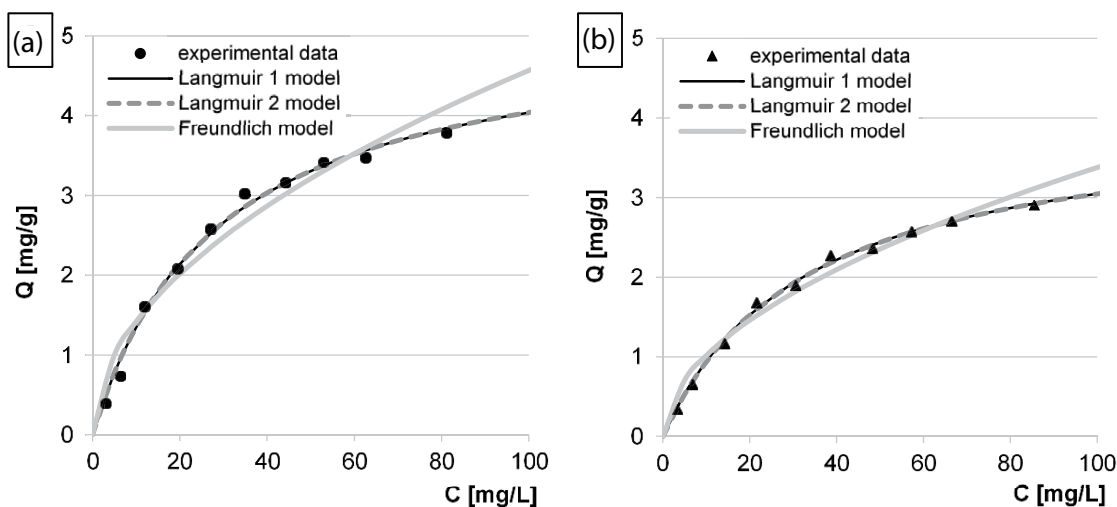


Fig. 5. Isotherms of sorption of (a) RB5 and (b) BR46 onto HF. Temperature 22°C.



Table 5  
Comparison of RB5 and BR46 sorption capabilities of various sorbents

Dye	Sorbent	$Q_{\max}$ [mg/g]	Sorption pH	Equilibrium time [h]	Source
Reactive Black 5	Coconut shells	0.82	2	1.0	[8]
	Pumpkin seed husks	0.96	2	3.0	[37]
	Sunflower biomass	1.10	2	3.5	[34]
	Sunflower seed husks	2.89	3	1.5	[29]
	Fly ashes	4.40	5.6	24	[40]
	Hen feathers	5.19	2	3.5	This work
	Active carbon from nut tree wood	19.30	5	6.7	[41]
	Powder activated carbon (commercial)	58.80	b.d	b.d	[42]
	Hen feathers	4.06	5	3.5	This work
	Wood sawdust	19.24	b.d	2.0	[43]
Basic Red 46	Bone meal	24.56	6	1.5	[44]
	<i>Paulownia tomentosa</i> tree leaves	43.1	8	70	[45]
	Rape seed husks	49.0	8	10	[46]
	Lemon skin	54.0	6	240	[38]
	Moroccan crude clay	54.0	6	0.33	[47]
	Active carbon from the <i>Cerbera</i> biomass	65.7	7	90	[48]
	Granular activated carbon	333.3	8	<1	[49]

than the plant biomass-based sorbents, similar to sawdust [43], tree leaves [45], or skins of citrus fruits [38], which probably stems from the lower number of acidic functional groups available on the surface of feathers. In contrast, HF exhibit a higher capability to bind RB5 dye than the lignocellulosic waste materials, such as pumpkin seed husks [37], sunflower seed husks [29,34], or coconut shells [8]. This may be attributable to the presence of alkaline (amine) functional groups in the feather structure that serve as the main sorption centers for anionic dyes. The number of active sites with the basic nature is usually low in the plant biomass, which explains the low RB5 sorption effectiveness (Table 5).

#### 4. Summary

Hen feathers (HF) can be used as a sorbent to remove both anionic and cationic dyes. Their maximal sorption capacity reached 5.19 mg/g for RB5 and 4.06 mg/g for BR46. The effectiveness of dye sorption onto HF largely depends on the initial solution pH. The highest sorption effectiveness of the anionic dye RB5 was achieved at pH 2, whereas that of the cationic dye BR46 - at pH 5. The HF was observed to cause significant changes in solution pH during the sorption process. The system tended to reach the pH value approximating their  $pH_{PZC}$ , that is,  $pH_{PZC} = 7.65$ . The physical sorption turned out to be the main mechanism of dye binding onto HF. The significant superiority of the physical sorption over chemisorption was indicated by the better fit of the pseudo-first order model than of the second-pseudo order model to the experimental data. Only one type of the sorption center was found to play the key role in dye sorption onto HF, as shown by the identical values of  $K_c$ ,  $K_1$ , and  $K_2$  constants determined from the Langmuir 1 and Langmuir 2 models. Presumably,

the protonated amine groups of keratin served as the main active centers for the anionic dye RB5, while the deprotonated carboxyl groups for the cationic dye BR46.

#### Acknowledgements

This study was financed under Project No. 18.610.008-300 of the University of Warmia and Mazury in Olsztyn, Poland.

#### References

- [1] C.R. Holkar, A.J. Jadhav, D.V. Pinjari, N.M. Mahamuni, A.B. Pandit, A critical review on textile wastewater treatments: possible approaches, *J. Environ. Manage.*, 182 (2016) 351–366.
- [2] A. Albahnasawi, E. Yüksel, E. Gürbulak, F. Duyum, Fate of aromatic amines through decolorization of real textile wastewater under anoxic-aerobic membrane bioreactor, *J. Environ. Chem. Eng.*, 8 (2020) 104226. <https://doi.org/10.1016/j.jece.2020.104226>.
- [3] M.R. Samarghandi, A. Dargahi, A. Shabanloo, H.Z. Nasab, Y. Vaziri, A. Ansari, Electrochemical degradation of methylene blue dye using a graphite doped  $PbO_2$  anode: optimization of operational parameters, degradation pathway and improving the biodegradability of textile wastewater, *Arab. J. Chem.*, 13 (2020) 6847–6864.
- [4] S. Arslan, M. Eyvaz, E. Gürbulak, E. Yüksel, A Review of State-of-the-Art Technologies in Dye-Containing Wastewater Treatment—The Textile Industry Case, In: *Textile Wastewater Treatment*, IntechOpen, 2016, pp. 1–28, doi: 10.5772/64140. Available at: <https://www.intechopen.com/books/textile-wastewater-treatment/a-review-of-state-of-the-art-technologies-in-dye-containing-wastewater-treatment-the-textile-industr>.
- [5] E.E. El-Katori, M.A. Ahmed, A.A. El-Bindary, A.M. Oraby, Impact of CdS/SnO<sub>2</sub> heterostructured nanoparticle as visible light active photocatalyst for the removal methylene blue dye, *J. Photochem. Photobiol. A Chem.*, 392 (2020) 112403. <https://doi.org/10.1016/j.jphotochem.2020.112403>.
- [6] H.A. Kiwaan, T.M. Atwee, E.A. Azab, A.A. El-Bindary, Photocatalytic degradation of organic dyes in the presence of nanostructured titanium dioxide, *J. Mol. Struct.*, 1200 (2020) 127115. <https://doi.org/10.1016/j.molstruc.2019.127115>.

- [7] C. Contescu, S. Adhikari, N. Gallego, N. Evans, B. Biss, Activated carbons derived from high-temperature pyrolysis of lignocellulosic biomass, *J. Carbon Res.*, 4 (2018) 1–16.
- [8] T. Józwiak, U. Filipkowska, P. Bugajska, T. Kalkowski, The use of coconut shells for the removal of dyes from aqueous solutions, *J. Ecol. Eng.*, 19 (2018) 129–135.
- [9] A. Almasi, S.A. Mousavi, A. Hesari, H. Janjani, Walnut shell as a natural adsorbent for the removal of Reactive Red 2 from aqueous solution, *Int. Res. J. Appl. Basic Sci.*, 10 (2016) 551–556.
- [10] S. Boumchita, A. Lahrichi, Y. Benjelloun, S. Lairini, V. Nenov, F. Zerrouq, Application of peanut shell as a low-cost adsorbent for the removal of anionic dye from aqueous solutions, *J. Mater. Environ. Sci.*, 8 (2017) 2353–2364.
- [11] S. Sawasdee, H. Jankerd, P. Watcharabundit, Adsorption of dyestuff in household-scale dyeing onto rice husk, *Energy Procedia*, 138 (2017) 1159–1164.
- [12] S. Banerjee, G.C. Sharma, R.K. Gautam, M.C. Chattopadhyaya, S.N. Upadhyay, Y.C. Sharma, Removal of Malachite Green, a hazardous dye from aqueous solutions using *Avena sativa* (oat) hull as a potential adsorbent, *J. Mol. Liq.*, 213 (2016) 162–172.
- [13] M.I. Mohamed, Anaam A. Sabri, Application of wheat husk in color removal of textile wastewater, *Eng. Technol. J.*, 37 (2019) 296–302.
- [14] D.P. Dutta, S. Nath, Low cost synthesis of SiO<sub>2</sub>/C nanocomposite from corn cobs and its adsorption of uranium (VI), chromium (VI) and cationic dyes from wastewater, *J. Mol. Liq.*, 269 (2018) 140–151.
- [15] I. Anastopoulos, G.Z. Kyzas, Agricultural peels for dye adsorption: a review of recent literature, *J. Mol. Liq.*, 200 (2014) 381–389.
- [16] A. Stavrinou, C.A. Aggelopoulos, C.D. Tsakiroglou, Exploring the adsorption mechanisms of cationic and anionic dyes onto agricultural waste peels of banana, cucumber and potato: adsorption kinetics and equilibrium isotherms as a tool, *J. Environ. Chem. Eng.*, 6 (2018) 6958–6970.
- [17] M.M.T. Namboodiri, K. Pakshirajan, Valorization of Waste Biomass for Chitin and Chitosan Production, In: *Waste Biorefinery*, 2020, Elsevier, pp. 241–266, doi: 10.1016/B978-0-12-818228-4.00010-1.
- [18] U. Filipkowska, T. Józwiak, P. Szymczyk, M. Kuczajowska-Zadrożna, The use of active carbon immobilised on chitosan beads for RB5 and BV10 dye removal from aqueous solutions, *Prog. Chem. Appl. Chitin Its Deriv.*, 22 (2017) 14–26.
- [19] A. Murcia-Salvador, J.A. Pellicer, M.I. Rodríguez-López, V.M. Gómez-López, E. Núñez-Delgado, J.A. Gabaldón, Egg by-products as a tool to remove direct blue 78 dye from wastewater: kinetic, equilibrium modeling, thermodynamics and desorption properties, *Materials (Basel)*, 13 (2020) 1–18.
- [20] M. El Haddad, R. Mamouni, R. Slimani, N. Saffaj, M. Ridaoui, S. ElAntri, S. Lazar, Adsorptive removal of reactive Yellow 84 dye from aqueous solutions onto animal bone meal, *J. Mater. Environ. Sci.*, 3 (2012) 1019–1026.
- [21] S. Sharma, A. Gupta, A. Kumar, Keratin: An Introduction BT - Keratin as a Protein Biopolymer, In: *Extraction from Waste Biomass and Applications*, Springer, Cham, 2019, doi: 10.1007/978-3-030-02901-2.
- [22] A. Ansarullah, R. Rahim, A. Kusno, B. Baharuddin, N. Jamala, Utilization of waste of chicken feathers and waste of cardboard as the material of acoustic panel maker, *IOP Conf. Ser. Earth Environ. Sci.*, 126 (2018) 1–7.
- [23] T. Tesfaye, B. Sithole, D. Ramjugernath, V. Chunilall, Valorisation of chicken feathers: characterisation of chemical properties, *Waste Manage.*, 68 (2017) 626–635.
- [24] A. Idris, R. Vijayaraghavan, U.A. Rana, D. Fredericks, A.F. Patti, D.R. MacFarlane, Dissolution of feather keratin in ionic liquids, *Green Chem.*, 15 (2013) 525–534.
- [25] S. Sharma, A. Gupta, S.M. Saufi, C.Y.G. Kee, P.K. Podder, M. Subramaniam, J. Thuraisingam, Study of different treatment methods on chicken feather biomass, *IJUM Eng. J.*, 18 (2017) 47–55.
- [26] J. Yao, Y. Liu, S. Yang, J. Liu, Characterization of secondary structure transformation of stretched and slenderized wool fibers with FTIR spectra, *J. Eng. Fibers Fabr.*, 3 (2008) 1–10.
- [27] G. Zhang, L. Senak, D.J. Moore, Measuring changes in chemistry, composition, and molecular structure within hair fibers by infrared and Raman spectroscopic imaging, *J. Biomed. Opt.*, 16 (2011) 1–7.
- [28] T.K. Saha, N.C. Bhoumik, S. Karmaker, M.G. Ahmed, H. Ichikawa, Y. Fukumori, Adsorption characteristics of Reactive Black 5 from aqueous solution onto chitosan, *Clean Soil Air Water*, 39 (2011) 984–993.
- [29] T. Józwiak, U. Filipkowska, S. Brym, L. Kopeć, Use of aminated hulls of sunflower seeds for the removal of anionic dyes from aqueous solutions, *Int. J. Environ. Sci. Technol.*, 17 (2020) 1211–1224.
- [30] M. Afsharnia, H. Biglari, A. Javid, F. Zabihi, Removal of Reactive Black 5 dye from aqueous solutions by adsorption onto activated carbon of grape seed, *Iran. J. Health Sci.*, 5 (2017) 48–61.
- [31] A. Elsagh, O. Moradi, A. Fakhri, F. Najafi, R. Alizadeh, V. Haddadi, Evaluation of the potential cationic dye removal using adsorption by graphene and carbon nanotubes as adsorbents surfaces, *Arab. J. Chem.*, 10 (2017) S2862–S2869.
- [32] N. Yeddou Mezenner, A. Hamadi, S. Kaddour, Z. Bensaadi, A. Bensmaili, Biosorption behavior of basic red 46 and violet 3 by dead pleurotus mutilus from single- and multicomponent systems, *J. Chem.*, 2013 (2013) 1–12. <https://doi.org/10.1155/2013/965041>.
- [33] D.P. Dutta, A. Rathore, A. Ballal, A.K. Tyagi, Selective sorption and subsequent photocatalytic degradation of cationic dyes by sonochemically synthesized nano CuWO<sub>4</sub> and Cu<sub>3</sub>Mo<sub>2</sub>O<sub>9</sub>, *RSC Adv.*, 5 (2015) 94866–94878.
- [34] J.F. Osma, V. Saravia, J.L. Toca-Herrera, S.R. Couto, Sunflower seed shells: a novel and effective low-cost adsorbent for the removal of the diazo dye Reactive Black 5 from aqueous solutions, *J. Hazard. Mater.*, 147 (2007) 900–905.
- [35] A. Fallis, Adsorption of reactive black 5 dye onto modified wheat straw: isotherm and kinetics study, *J. Chem. Inf. Model.*, 53 (2013) 1689–1699.
- [36] M.C. Ribas, M.A. Adebayo, L.D.T. Prola, E.C. Lima, R. Cataluña, L.A. Feris, M.J. Puchana-Rosero, F.M. Machado, F.A. Pavan, T. Calvete, Comparison of a homemade cocoa shell activated carbon with commercial activated carbon for the removal of reactive violet 5 dye from aqueous solutions, *Chem. Eng. J.*, 248 (2014) 315–326.
- [37] A. Kowalkowska, T. Józwiak, Utilization of pumpkin (*Cucurbita pepo*) seed husks as a low-cost sorbent for removing anionic and cationic dyes from aqueous solutions, *Desal. Wat. Treat.*, 171 (2019) 397–407.
- [38] T. Józwiak, U. Filipkowska, P. Zajko, Use of citrus fruit peels (grapefruit, mandarin, orange, and lemon) as sorbents for the removal of basic violet 10 and basic red 46 from aqueous solutions, *Desal. Wat. Treat.*, 163 (2019) 385–397.
- [39] W.K. Elwira TOMCZAK, Modelowanie kinetyki sorpcji z zastosowaniem pochodnych ułankowych dla układu barwnik azowy – sorbent roślinny, *INŻYNIERIA I Apar. Chem.*, 52 (2013) 376–377.
- [40] P. Pengthamkeerati, T. Satapanajaru, N. Chatsatapattayakul, P. Chairattananamanokorn, N. Sananwai, Alkaline treatment of biomass fly ash for reactive dye removal from aqueous solution, *Desalination*, 261 (2010) 34–40.
- [41] B. Heibati, S. Rodriguez-Couto, A. Amrane, M. Rafatullah, A. Hawari, M.A. Al-Ghouti, Uptake of Reactive Black 5 by pumice and walnut activated carbon: chemistry and adsorption mechanisms, *J. Ind. Eng. Chem.*, 20 (2014) 2939–2947.
- [42] Z. Eren, F.N. Acar, Adsorption of Reactive Black 5 from an aqueous solution: equilibrium and kinetic studies, *Desalination*, 194 (2006) 1–10.
- [43] L. Laasri, M.K. Elamrani, O. Cherkaoui, Removal of two cationic dyes from a textile effluent by filtration-adsorption on wood sawdust, *Environ. Sci. Pollut. Res.*, 14 (2007) 237–240.
- [44] S.L.M. El Haddad, R. Slimani, R. Mamouni, S. Nabil, M. Ridaoui, Adsorptive removal of a cationic dye – basic red 46 from aqueous solutions using animal bone meal, *J. Eng. Stud. Res.*, 18 (2012) 43–51.

- [45] F. Deniz, S.D. Saygideger, Removal of a hazardous azo dye (Basic Red 46) from aqueous solution by princess tree leaf, *Desalination*, 268 (2011) 6–11.
- [46] N.M. Mahmoodi, M. Arami, H. Bahrami, S. Khorramfar, Novel biosorbent (Canola hull): surface characterization and dye removal ability at different cationic dye concentrations, *Desalination*, 264 (2010) 134–142.
- [47] A.B. Karim, B. Mounir, M. Hachkar, M. Bakasse, A. Yaacoubi, Removal of Basic Red 46 dye from aqueous solution by adsorption onto Moroccan clay, *J. Hazard. Mater.*, 168 (2009) 304–309.
- [48] N.A.I. Azmi, N.F. Zainudin, U.F.M. Ali, Adsorption of basic Red 46 using sea mango (*Cerbera odollam*) based activated carbon, *AIP Conf. Proc.*, 1660 (2015) 1–16.
- [49] H.N. Abdul Halim, K.L.K. Mee, Adsorption of Basic Red 46 by granular activated carbon in a fixed-bed column, *Int. Conf. Environ. Ind. Innov.*, 12 (2011) 263–267.